Journal of
Ship&Ocean
Technology
© SEPTEMBER 1999

SOTECH Vol.3, No.3; pp.1~12

Assessment of the Effect of Probabilistic Modeling of Sea-States in Fatigue Damage Calculations

Rasmus Folsϕ, Mario Dogliani

Registro Italiano Navale(RINA), New Products and Research Department, via Corsica 12, 16128 Genova, Italy

Abstract

Spectral fatigue damage calculations has been performed on four ships in order to assess the effect that the probabilistic modeling of sea states has on the estimated fatigue life. The damage estimation method is based on the Miner-Palmgren fatigue damage formulation and a spectral approach is used to determine the necessary variances of the stress processes. Both the horizontal and vertical hull girder bending induced stress process together with the local water pressure induced stress process is taken into account. Ten wave scatter diagrams are applied in the calculations and their fatigue severity is assessed by analyzing the results obtained with the ten scatter diagrams and the four ships. All four ships are analyzed both in full load and ballast conditions and while traveling at both full and reduced speed. It is found that the fatigue severity of a wave scatter diagram is dependent on several parameters, some of these being the extreme wave height extrapolated from the scatter diagram and the mean zero up-crossing period in conjunction with the ship length. Based on these three parameters an expression is derived in order to calculate one single number describing the fatigue severity of a scatter diagram with respect to a certain ship.

Keywords : fatigue damage, fatigue severity, wave environments, spectral analysis

1 Introduction

Classification societies have the recent years acknowledged that fatigue of structural elements in ship structures presents a problem that must be taken into account both in the design and the maintenance of ships. Extensive work have therefore been carried out within the societies in order to develop a set of rules that can be applied in the assessment of a ship's fatigue reliability. During this work the problem of selecting a wave environment suitable for application to design fatigue life calculations has occurred.

It is generally accepted that the North Atlantic is one of the most severe ocean areas in the world when ultimate loads are considered. But when fatigue damage is considered it has quite often been pointed out in the literature that the North Atlantic is not necessarily among the most severe ocean areas in the world. An example of this is a paper by Chen and Thayamballi[Chen

et al., 1991]. In this paper a comparison of the fatigue severity of all GWS, *Global Wave Statistics*[Hogben et al., 1986], areas has been conducted. A fatigue severity parameter has been calculated for each GWS zone where after these has been normalized with the fatigue severity parameter obtained from a composite wave scatter diagram representing the New York - Rotterdam route, which could be interpreted as representing the North Atlantic. The results of this are shown in Figure 15 in Chen's paper, and it is quite clearly observed that the New York - Rotterdam route is not among the most severe wave environments in the world, when fatigue is considered. However, Soares and Moan[Guedes Soares et al., 1991] also made fatigue considerations and concluded that the North Atlantic and the North Sea are the most severe areas in the world, whereas Bitner-Gregersen et al.[Bitner-Gregersen et al., 1993] have pointed out that the severity of a certain wave environment is dependent on the characteristics of the considered ship.

Within a significant rule calibration task undertaken by RINA, spectral fatigue damage calculations have been performed in order to compare the fatigue severity of ten composite wave scatter diagrams, one of these being based on four North Atlantic GWS areas, with respect to four ships of different sizes. Based on the results of these calculations an analytical expression, describing the fatigue severity of a given wave scatter diagram with respect to a certain ship, is sought for. If it is possible to develop such an expression it will be very easy to evaluate which wave environments are most severe to a certain ship and which environments are mild.

2 Fatigue Damage Accumulation Model

Based on the assumption that the fatigue damage is linearly accumulative, the fatigue damage due to a stochastic load process, with N stress cycles, can be calculated with the Miner-Palmgren model as

$$D = \frac{N}{K} E\{\Delta\sigma^m\} = \frac{N}{K} \int_0^\infty \Delta\sigma^m f_\sigma(\Delta\sigma) d\Delta\sigma \tag{1}$$

where

D - accumulated fatigue damage ($D = 1$: failure)
m - slope parameter in S-N curve
K - scale parameter in S-N curve
$\Delta\sigma$ - stress range

If it is assumed that the load process is Gaussian, the probability distribution of the stress ranges can be described with a Rayleigh distribution, where the expected value is given as

$$E\{\Delta\sigma^m\} = b^m \Gamma\left(1 + \frac{m}{2}\right) \tag{2}$$

where $b = 2\sqrt{2m_o}$, where m_o is the 0'th spectral moment (variance) of the process. The n'th spectral moment of the process will in this study be calculated in the following manner, which includes the effect of wave spreading

$$m_n(H_S, T_Z, \overline{\psi}) = \int_0^\infty \int_{\overline{\psi}-\frac{\pi}{2}}^{\overline{\psi}+\frac{\pi}{2}} \phi_\sigma(\psi, \omega)^2 S_{\omega\nu}(H_S, T_Z, \omega) \omega^n D(\psi) d\psi d\omega \tag{3}$$

where $\phi_\sigma(\psi, \omega)$ is the stress response amplitude operator(RAO), $S_{\omega\nu}(H_S, T_Z, \omega)$ is the wave spectrum and $D(\psi)$ is the frequency independent spreading function that accounts for short crestedness about the mean angle of encounter $\overline{\psi}$, defined as the angle between the ship heading and the mean wave direction. The number of stress cycles N in each sea state are estimated based on the time period t_l, over which the damage will be accumulated, the zero up-crossing frequency of the response $\nu_o(T_Z, \overline{\psi})[s^{-1}]$ and the joint probabilities $f(H_S, T_Z, \theta)$, describing the probability of the considered sea state, which are obtained from a scatter diagram. H_S, T_Z and θ denotes respectively the significant wave height, the zero up-crossing period and the prevailing wave direction.

2.1 Stress Transfer Functions

The method applied in the present study for calculating the stress transfer functions and the spectral moments of the response specters are thoroughly described by Folsϕ[Folsϕ, 1998]. The method is based on the horizontal and vertical bending transfer functions for the global stress process and the side shell pressure transfer functions for the local stress process induced by the external water pressure. Above the mean waterline MWL the two global stress processes are combined to one set of stress transfer functions in the traditional way. Below the waterline the two global stress processes are combined with the local stress process in the traditional way for fully submerged longitudinals, whereas for longitudinals located sometimes above the sea surface and sometimes below, the total combined stress transfer functions are determined numerically. This is done in order to include the effect of the alternating wet & dry areas, which is quite significant for longitudinals located close to the MWL, see [Folsϕ, 1998].

The bending moment RAO's can be obtained in various ways. In the present study a linear strip theory program, SGN80[Pittaluga et al., 1984], based on the theory developed by Salvesen et al.[Salvesen et al., 1970] is applied. Alternatively a program based on the quadratic strip theory presented by Jensen and Pedersen[Jensen et al., 1979] could have been applied. However, this theory has the drawback that only motions and forces in the vertical plane are considered, which means that the horizontal bending can not be included in the fatigue life predictions. Furthermore Jensen and Dogliani[Jensen et al., 1996] has made fatigue calculations based on the quadratic strip theory and concluded that the non-linearity's included in this theory only has a minor importance for the fatigue damage. A third approach is to apply a 3D code[Lin et al., 1997] and [WADAM, 1990]. However, this is quite time consuming, and therefore not considered feasible in the present study where a very large amount of calculations have been performed.

In the present study the pressure transfer functions are calculated by the linear strip theory program SGN80, according to the method described by Caretti[Caretti, 1979], but also these could have been obtained by applying a 3D code, as done by Cramer et al.[Cramer et al., 1993].

3 Effect of the Probabilistic Modeling of Sea States

As part of the rule calibration task carried out by RINA, the main goal with the study described here was to perform systematic calculations in order to assess the effect that the probabilistic modeling of sea states has on the estimated fatigue life of typical ship structural details. To fulfill this goal four ships has been chosen from the extensive collection of ships classed by RINA. The four ships are all tankers with main particulars as shown in Table 1

The probabilistic modeling of sea states is embedded in the choice of scatter diagram. The

Table 1. Main particulars of the four analyzed ships.

		TANKER 1	TANKER 2	TANKER 3	TANKER 4
Length L_{pp} $[m]$		109.0	182.0	264.0	330.7
Breadth $[m]$		17.5	27.4	45.1	51.8
Draft laden $[m]$	$Aft.$	7.95	11.28	17.10	16.38
	$Fore$	6.92	11.28	17.10	16.38
Draft ballast $[m]$	$Aft.$	5.10	8.34	8.24	9.36
	$Fore$	3.36	6.27	6.60	9.36
Displacement laden	$[T]$	11460	46990	172400	234300
Displacement ballast	$[T]$	6169	29420	79910	130200
	Sectional Properties of Midship Sections				
Neutral axis from BL	$[m]$	4.06	7.15	10.81	12.64
Moment of inertia I_{yy}	$[m^4]$	16.45	106.00	536.6	1052.0
Moment of inertia I_{zz}	$[m^4]$	37.20	226.10	1514.0	2522.0

scatter diagram essentially assigns different probabilities to a range of sea states, characterized by the significant wave height H_S and the zero up-crossing period T_Z. In order to perform the assessment of the effect of probabilistic modeling of sea states, 10 scatter diagrams have been constructed by the use of *Global Wave Statistics - PC Version*. The scatter diagrams have been constructed based on two different 'concepts'. The 'geographical' concept, where the scatter diagram is composed from wave data from one specific geographical area, and the 'seasons' concept where the scatter diagram is composed from wave data gathered from one seasonal zone. With seasonal zones is referred to the division of the worlds ocean surface into zones according to the 'International Load Line Convention'. Some of these zones are classified as being one season all year(e.g. areas which are "summer" all the year), while others, so called 'seasonal zones', are classified as being one season one part of the year and another season the rest of the year(e.g. they are "winter" for a certain period of the year and "summer" for others). This was accounted for by using the appropriate seasonal scatter diagram for the latter areas, hence the seasonal scatter diagrams below, Winter, Summer, North Atlantic Summer and Tropical, are composed of wave data gathered only in the appropriate period of the year. The 'geographical' scatter diagrams are composed of wave data gathered all through the year. The ten scatter diagrams are as follows

1. North Atlantic, based on *GWS* areas 8,9,15,16.
2. South Atlantic, based on *GWS* areas 87, 88, 89, 96, 97, 98.
3. North Pacific, based on *GWS* areas 7, 12, 13, 20, 21, 30.
4. South Pacific, based on *GWS* areas 86, 102 (94 contains insufficient data).
5. North Sea, based on *GWS* area 11.
6. Mediterranean, based on *GWS* area 26 and 27
7. Winter, based on all *GWS* areas within the seasonal winter zone. Only wave data gathered in the winter period is considered.
8. Summer, based on all *GWS* areas within the seasonal summer, and summer zones. Only wave data gathered in the summer period is considered.
9. Tropical, based on all *GWS* areas within the seasonal tropical, and tropical zones. Only wave data gathered in the tropical period is considered.

Table 2. Classification of scatter diagrams.

ZERO UP-CROSSING PERIOD		EXTREME WAVE HEIGHT	
Scatter diagram	$T_Z[s]$	Scatter diagram	$H_{ext}[m]$
Mediterranean	5.42	Tropical	12.02
North Sea	6.15	North Atl. Summer	15.34
Tropical	6.94	Mediterranean	17.00
North Atl. Summer	7.44	Summer	19.14
Summer	7.79	South Pacific	20.56
North Pacific	8.12	North Sea	20.70
South Atlantic	8.22	North Pacific	21.16
South Pacific	8.24	South Atlantic	21.18
North Atlantic	8.40	North Atlantic	22.38
Winter	8.45	Winter	22.66

10. North Atlantic summer, based on *GWS* areas 33, 34 and 35

For all wave scatter diagrams a uniform distribution of directions were applied.

3.1 Tentative Classification of Wave Scatter Diagrams

The severity of a certain scatter diagram can be measured in different ways. Here, two different approaches will be applied. The first of these is a classification of the scatter diagrams based on their mean zero up-crossing period, the second is a classification based on the extreme wave height extrapolated from the scatter diagram. The extreme wave height is determined as the wave height with a probability of exceeding of 10^{-5}. The two classifications are shown in Table 2.

In Section 3.3 it will be examined whether one of these classifications is better than the other, or if another classification method is needed.

3.2 Results of Calculations

The fatigue damage both in the deck - transverse webframe connection and in the side shell longitudinal - transverse webframe connection has been calculated for all four ships in both ballast and full load condition at two different speeds, full speed and 0.6 of full speed, and for all ten wave scatter diagrams, in total 320 damage estimates. The damage induced in the side shell connection is calculated for a longitudinal placed approximately one meter below the waterline in both loading conditions.

In the following some trends which can be deduced from the results will be pointed out and visualized as far as possible.

The first trend that can be observed is that, as expected, the scatter diagrams with relatively short waves(low mean T_Z) causes more damage in the small ships than in the large ships, whereas when scatter diagrams with relatively long waves are considered, more damage is induced in the large ships. This trend can not immediately be observed from the results, because the different structural geometry in the four ships means that the damage estimates for the four ships can't be compared without including an effect of this. In the present study it is not interesting to compare

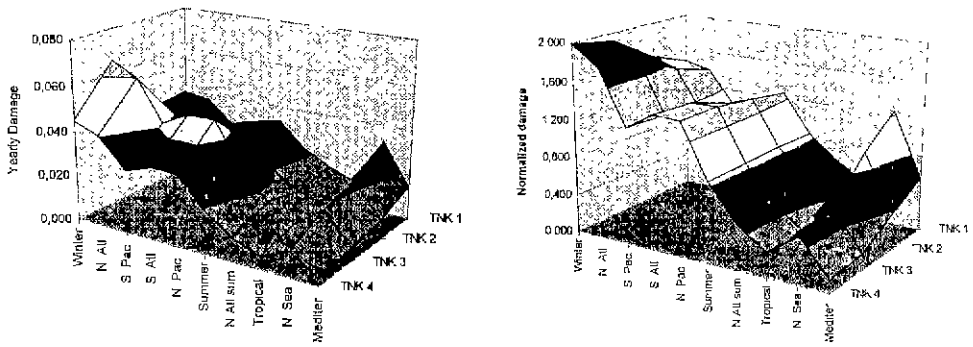

Figure 1. Yearly and normalized damage at the deck for the four ships in full load condition at full speed. in all ten scatter diagrams.

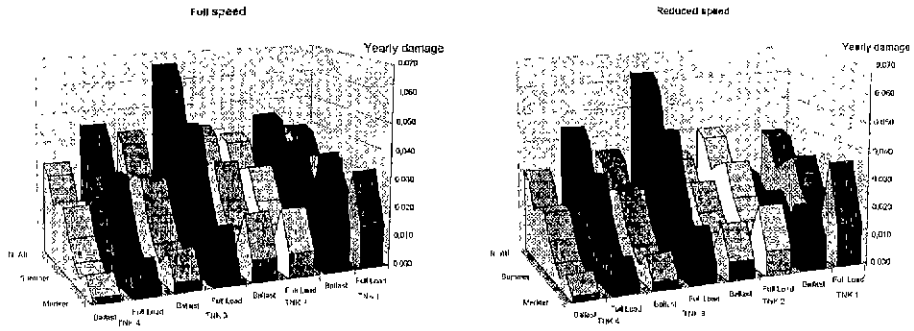

Figure 2. Yearly damage in the deck of the four considered ships in full load and ballast condition, for both full and reduced speed and all 10 scatter diagrams.

the ships including the different structural geometry, as only the dependency between ship size and probabilistic modeling of sea states is sought after. Therefore the effect of the different structural geometry has been filtered out by normalizing all the damage estimates with the mean damage estimate for that particular ship. The effect of this can be seen in Figure 1.

From the plot with the normalized damage estimates the before mentioned trend is clearly observed. However, it should be noted that even for the small ships the North Atlantic and Winter scatter diagrams with the relatively long waves are more severe than the scatter diagrams with short waves. As regards the calculations performed in ballast condition and the calculations with reduced speed, in both loading conditions, the same trends can be observed, except that for the calculations at reduced speed it is found that the North Sea scatter diagram is just as severe to Tanker 1 as the Winter and North Atlantic scatter diagrams are. When the damage in the side shell is considered it is seen that all the same trends can be observed, except that it is now clear that the North Sea scatter diagram is the most severe to Tanker 1 in all conditions.

The second observed trend is that the fatigue damage generally is smaller in ballast condition than in full load condition, except for the damage in the deck of the small ships traveling at full speed, see Figure 2 and Figure 3.

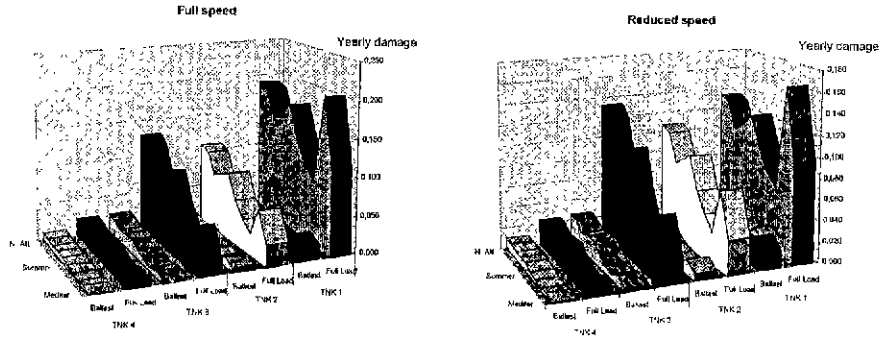

Figure 3. Yearly damage in the side shell of the four considered ships in full load and ballast condition, for both full and reduced speed and all 10 scatter diagrams.

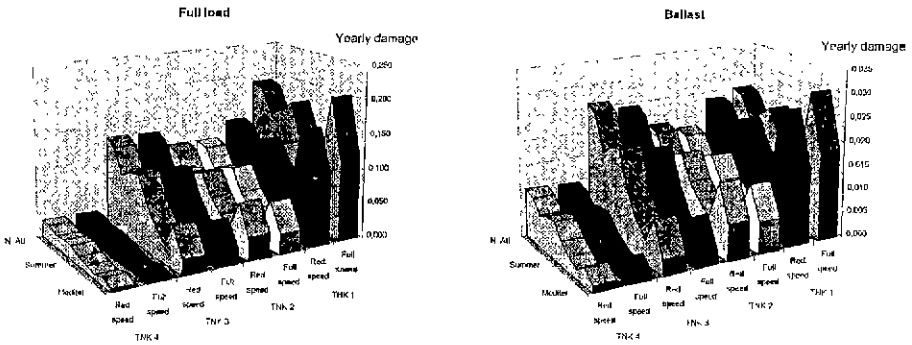

Figure 4. Yearly damage in the side shell of the four ships for both reduced and full speed, full load and ballast conditions and all 10 scatter diagrams.

Another interesting thing that can be seen from Figure 3 is that the damage in the side shell seems to be less severe for the large ships than for the smaller ships. This could be because the pressure loads from the external water doesn't increase much when the ship size is increased, whereas the scantlings of the structural members in the side shell increases considerably due to the increasing global loads on the hull structure.

The third trend is that for the large/medium ships more damage is induced in the side shell when traveling at reduced speed than at full speed, see Figure 4. This is quite surprising and no explanation has been found for this. However, this has also been observed by Friis Hansen and Winterstein[Friis Hansen et al., 1995] who analyzed a tanker with $L_{PP} = 262.13\ m$.

3.3 Corrected Classification of Wave Scatter Diagrams

From the illustrations in the previous section it can be seen that the classification of scatter diagrams based on the mean zero up-crossing period doesn't seem to reflect the fatigue severity of the scatter diagrams very well. Furthermore it is also clearly seen that the severity of a certain scatter diagram is not only dependent on characteristics of the scatter diagram, but also on the character-

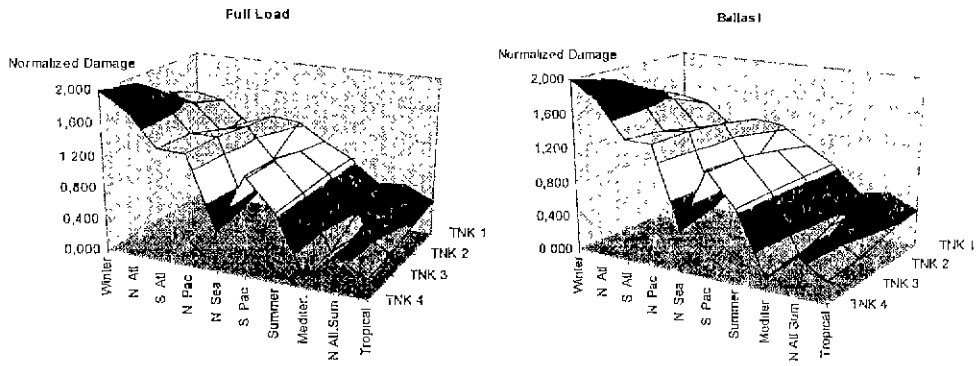

Figure 5. Normalized damage at the deck of the four ships in full load and ballast conditions at full speed, evaluated with all 10 scatter diagrams classified by extreme wave height.

istics of the ship which is being examined. In Figure 5 it is shown that the classification of scatter diagrams based on the extreme wave height describes the severity with equally little accuracy as the mean-period classification. Therefore another classification method is needed, in order to have a reliable method to compare the severity of different scatter diagrams without actually performing the time demanding fatigue calculations with all scatter diagrams.

One way to make a new classification could be to assume the classification based on extreme wave heights, and then correct this with respect to the mean frequency of the scatter diagram and the length of the considered ship. It is clear that when the wave lengths are approximately of the same length as the ship length, the induced wave loads will increase. Therefore the extreme wave heights could be corrected in the following way, which ensures that the fatigue severity(H_{cor}) is decreased more when the wave lengths is farther from the ship length

$$H_{cor} = H_{ext} - \frac{|L_{PP} - \lambda|}{\lambda} \tag{4}$$

The question is now on what period the wave length shall be based. It has during this study been found that the best results are obtained when the wave length in the denominator is based on the mean zero up-crossing period, while the period in the nominator is based on the mean peak period, which is obtained as 1.41 times T_Z(note that although true only for Pierson Moskowitz spectrum, this is a largely accepted approximation), which then for wave lengths must be squared, yielding a factor $\simeq 2$. Finally some factors tuning the value of the correction subtracted from the extreme wave height is added. These factors are obtained by fitting equation (4) to the result from the direct calculation. However, in order to achieve satisfactory results for the classification with respect to both the deck and the side damage, two expressions are necessary. For the deck damage:

$$H_{cor} = H_{ext} - 1.5\left(\frac{|L_{PP} - 2.1\lambda_Z|}{\lambda_Z}\right)^{1.3} \tag{5}$$

and for the side damage:

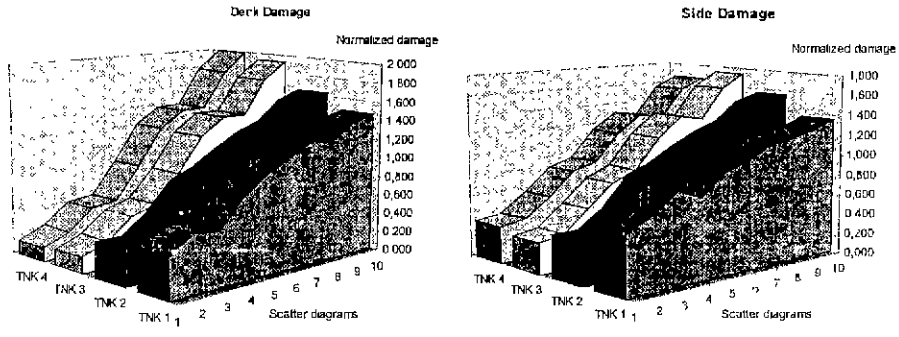

Figure 6. Normalized damage at the deck and in the side shell of the four ships in full load condition at full speed, evaluated with all 10 scatter diagrams classified by *corrected* extreme wave height.

$$H_{cor} = H_{ext} - 2\left(\frac{|L_{PP} - 2.3\lambda_Z|}{\lambda_Z}\right)^{1.2} \tag{6}$$

where λ_Z - wave length based on mean zero up-crossing period.

By classifying the scatter diagrams based on H_{cor} instead of H_{ext} a more correct classification is achieved, see Figure 6. The corrected scatter diagram classifications and the calculated H_{cor} values are for each ship shown in Table 3.

It can be seen that the classification of scatter diagrams are quite different for the smaller ships, whereas the classifications for the two largest ships are identical, both with respect to side and deck damage. It is also seen that there are some resemblance's between the classifications for all four ships, for instance that the Winter scatter diagram is for all ships classified as the most severe, except for the side damage in Tanker 1 where the North Sea is classified as the most severe. Note also how the severity of the North Sea scatter diagram is very dependent on the ship size, going from being very severe to the smallest ship to being among the mild scatter diagrams for the longer ships. Furthermore it is seen that the classifications based on the side and the deck damage are alike except for Tanker 1. These trends are in accordance with the trends that can be deducted from the results of the calculations. However, equations (5) and (6) have been developed based on the calculation results, and therefore the good agreement could be expected. Therefore it is interesting to test the two equations on other results obtained for different scatter diagrams. To this purpose the results presented by Bitner-Gregersen et al.[Bitner-Gregersen et al., 1993] have been used, especially reference is made to Table 5 of that paper, which contains estimated annual accumulated fatigue damages for 25 GWS areas. For each of these areas *GWS PC-version* has been consulted and the 10^{-5} extreme wave height and the mean zero up-crossing period have been calculated in order to determine the H_{cor} for a ship with $L_{PP} = 250\ m$, identical to the length of the ship analyzed by Bitner- Gregersen et al. In Table 4 the classification of the scatter diagrams according to the results presented by Bitner-Gregersen et al. are compared to the classification obtained by the use of equation (5). It is seen that a good agreement is achieved, although there

Table 3. Corrected classifications of scatter diagrams.

TANKER 1	H_{cor}	TANKER 2	H_{cor}	TANKER 3	H_{cor}	TANKER 1	H_{cor}
			DECK DAMAGE				
Tropical	11,16	Tropical	11,68	Mediter.	8,92	Mediter.	4,51
N.Atl.Sum	14,15	Mediter.	13,63	Tropical	9,67	Tropical	7,60
Mediter.	16,72	N.Atl.Sum	15,34	N.Atl.Sum	13,93	N.Atl.Sum	12,29
Summer	17,74	Summer	18,98	N. Sea.	16,10	N. Sea.	13,07
S. Pac.	18,92	N. Sea.	19,24	Summer	18,22	Summer	16,83
S. Atl.	19,55	S. Pac.	20,13	S. Pac.	20,12	S. Pac.	19,02
N. Pac.	19,58	S. Atl.	20,76	N. Pac.	20,60	N. Pac.	19,43
N. Sea.	20,45	N. Pac.	20,80	S. Atl.	20,72	S. Atl.	19,61
N. Atl.	20,66	N. Atl.	21,85	N. Atl.	22,07	N. Atl.	21,07
Winter	20,92	Winter	22,10	Winter	22,39	Winter	21,42
			SIDE DAMAGE				
Tropical	10,37	Tropical	11,86	Mediter.	8,16	Mediter.	3,52
N.Atl.Sum	13,25	Mediter.	13,31	Tropical	9,50	Tropical	7,15
Summer	16,78	N.Atl.Sum	15,06	N.Atl.Sum	13,91	N.Atl.Sum	12,01
Mediter.	16,91	Summer	18,52	N. Sea.	15,64	N. Sea.	12,33
S. Pac.	17,89	N. Sea.	19,22	Summer	18,29	Summer	16,67
S. Atl.	18,52	S. Pac.	19,51	S. Pac.	20,29	S. Pac.	18,98
N. Pac.	18,57	S. Atl.	20,15	N. Pac.	20,75	N. Pac.	19,37
N. Atl.	19,61	N. Pac.	20,22	S. Atl.	20,89	S. Atl.	19,57
Winter	19,86	N. Atl.	21,19	N. Atl.	22,26	N. Atl.	21,07
N. Sea.	19,92	Winter	21,43	Winter	22,58	Winter	21,43

are some discrepancies. Especially it can be noted that the 5 most severe scatter diagrams identified by Bitner-Gregersen et al. are also identified as the 5 most severe scatter diagrams when equation (5) is applied. The same can be noted about the 9 least severe scatter diagrams, but not about the 5 least severe because there are some differences in the estimated severity of some of the milder scatter diagrams. In Table 4 the calculated values of H_{cor} are also shown for the 4 previously analyzed tankers.

Based on the above it seems fair to conclude that equations (5) and (6) with success can be used to make a preliminary evaluation of a wave scatter diagrams severity, with respect to fatigue damage, compared to the severity of other scatter diagrams.

4 Conclusions

Numerous fatigue damage calculations have been carried out for four ships and with ten wave scatter diagrams. Based on the results from these calculations it can be concluded that the fatigue severity of a certain wave scatter diagram is strongly dependent on the characteristics of the ship being considered. It can also be concluded that the interactions between wave scatter diagram, ship size, ship speed and loading condition is not very straightforward. An analytical expression for the evaluation of a scatter diagrams fatigue severity has been derived, and it has been showed to yield results which are in agreement with the results of the calculations. Furthermore, based on

the calculations it can also be concluded that the North Atlantic is severe not only when ultimate loads are considered, but also for fatigue damage, whereas the severity of the North Sea is strongly dependent on the ship size, and is thus found to be very severe for small ships and mild for large ships.

Acknowledgements

For the first author, this work has been financed by the European Commission through a Marie Curie Research Training Grant in the framework of the Industrial and Materials Technologies program. The financial support is gratefully acknowledged.

Table 4. Classification of 25 GWS scatter diagrams, ordered according to the damages estimated by Bitner-Gregersen et al. (column 2) and compared to the classification obtained by the use of eq. (5) (column 3 & 4). Furthermore the results obtained for the four previously analyzed tankers are shown.

		H_{cor}	CLASSI-	H_{cor}			
GWS	ELZ. DAM.	L_{PP}: 250	FICATION	TANK. 1	TANK. 2	TANK. 3	TANK. 4
AREA		EQ. (5)	EQ. (5)	L_{PP}: 109	L_{PP}: 182	L_{PP}: 264	L_{PP}: 330,7
100	0,304	23,949	1	22,065	23,194	23,938	23,190
94	0,281	21,785	4	19,900	21,020	21,821	21,111
97	0,240	21,551	5	19,709	20,860	21,445	20,608
9	0,227	22,189	2	20,514	21,692	22,045	21,100
103	0,227	22,172	3	20,528	21,710	22,024	21,061
98	0,217	20,798	9	18,936	20,083	20,701	19,882
95	0,211	21,238	7	19,376	20,523	21,141	20,322
12	0,181	21,385	6	20,720	21,962	21,130	19,720
101	0,177	21,159	8	19,645	20,842	20,992	19,960
7	0,176	20,037	13	18,456	19,646	19,879	18,882
30	0,164	20,684	10	19,363	20,579	20,493	19,367
13	0,160	20,337	12	18,929	20,137	20,156	19,071
102	0,152	20,538	11	19,094	20,298	20,362	19,295
85	0,146	17,617	16	16,036	17,226	17,459	16,462
4	0,112	19,494	15	19,492	20,645	19,184	17,514
96	0,100	19,968	14	19,685	20,910	19,681	18,119
43	0,092	15,925	18	15,016	16,255	15,692	14,384
73	0,071	11,221	24	10,147	11,379	11,004	9,766
45	0,062	12,572	21	11,775	13,016	12,330	10,974
72	0,055	11,899	23	11,303	12,545	11,638	10,200
70	0,049	11,930	22	11,570	12,802	11,649	10,117
40	0,046	14,974	19	18,064	17,294	14,434	11,638
11	0,045	16,683	17	20,447	19,235	16,093	13,055
22	0,041	13,747	20	14,734	15,317	13,360	11,322
71	0,012	6,591	25	11,226	9,444	5,937	2,581

References

1. Chen, Y.N., Thayambaili, Y.K., 1991, Consideration of Global Climatology and Loading Characteristics in Fatigue Damage Assessment of Ship Structures, Marine Structural Inspection, Maintenance and Monitoring Symposiom, Session VI - paper D. Ship Structure Comitee & The Society of Naval Architects and Marine Engineers
2. Folsϕ, R., 1998, Spectral Fatigue Damage Calculations in the Side Shells of Ships, With Due Account Taken to the Effect of Alternating Wet & Dry Areas, Marine Structures, Vol.11, pp.319-343
3. Hogben, N., DaCunha, L.F., Olliver, N.H., 1986, Global Wave Statistics, Brown Union Pub., London
4. Guedes Soares, C., Moan T., 1991, Model Uncertainty in the Long-term Distribution of Wave-induced Bending Moments For Fatigue Design of Ship Structures, Marine Structures, Vol.4, pp.295-315
5. Bitner-Gregersen, E.M., Cramer, E.H., Loseth, R., 1993, Uncertainties of Load Characteristics and Fatigue Damage of Ship Structures, OMAE - Volume II, Safety and Reliability, pp.211-218
6. Pittaluga, A., Bisagno, M., 1984, SGN-80 Moderne Techniche di Analisi del Comportamento in Mare, Convegno Nazionale di Ricerca Navale e Marina - NAV84 - Venezia 28-30 Novembre 1984 Sessione 7: Architettura / Seakeeping, Memoria n.2(in Italian)
7. Salvesen, N., Tuck, E.O., Faltinsen, O., 1970, Ship Motions and Sea Loads, Trans. SNAME, vol.78, pp.250-287
8. Jensen, J.J., Pedersen, P.T., 1979, Wave Induced Bending Moments in Ships - A Quadratic Theory, The Royal Institution of Naval Architects, 121, pp.151-165
9. Jensen, J.J., Dogliani, M., 1996, Wave Induced Ship Hull Vibrations in Stochastic Seaways, Marine Structures, Vol.9, pp.353-387
10. Lin, W.M., Shin, Y.S., Chung, J.S., Zhang, S., Salvesen, N., 1997, Nonlinear Predictions of Ship Motions and Wave Loads for Structural Analysis, OMAE 1997 - Volume I-A, Offshore Technology, pp.243-250
11. WADAM, 1990, Wave Loading by Diffraction and Morison Theory, Technical Report, Det Norske Veritas Sesam Systems Hlvik, Norway, 1990, Sesam Users Manual
12. Friis Hansen, P., Winterstein, S.R., 1995, Fatigue Damage in the Side Shells of Ships, Marine Structures, Vol.8. pp.631-655
13. Caretti, F., 1979, Report No. 200, Registro Italiano Navale, Genova, Italy(in Italian)
14. Cramer, E.H., Loseth, R., Bitner-Gregersen, E., 1993, Fatigue in Side Shell Longitudinals Due to External Wave Pressure, OMAE 1993 - Volume II, Safety and Reliability, pp.267-272